Theory of Onset in Magnetoplasmadynamic Thrusters

J.L. Lawless* and V.V. Subramaniam†
Carnegie-Mellon University, Pittsburgh, Pennsylvania

The one-dimensional self-field flow in magnetoplasmadynamic (MPD) thrusters is analyzed in the frozen- and equilibrium-flow limits. The theory explains the behavior of efficiency and predicts a new mechanism for the destructive "onset" phenomenon. This model predicts that smoothly accelerating supersonic flow can exist only below a critical current level because of a back-EMF effect. This limit is interpreted as onset and correlates with the conventional $J^2/\dot{m}$ parameter.

Nomenclature

a = acoustic speed of sound
$\mathcal{R}$ = aspect ratio = W/H
B = magnetic field
B_i = magnetic field at the inlet, $x=0$
E = electric field
F = ρu = mass flux
H = interelectrode distance
h = enthalpy per unit mass
J = total current
j = current density
k_b = recombination rate constant
k_f = ionization rate constant
L = thruster length
M = Mach number = u/a
$\dot{m}$ = mass flow rate
m_A = atomic mass
P = pressure
T = temperature
T_h = total thrust at the exit, $x=L$
u = flow speed in x direction
u_i = inlet flow speed
V = voltage drop across the thruster
V_s = sum of the sheath voltage drops
W = width of the electrode transverse to the flow
x = coordinate in the flow direction
α = ionization fraction
η = overall performance efficiency
κ = B_i/B^*
ρ = mass density
σ = electrical conductivity
ϵ_i = first ionization energy
η_L = Lorentz efficiency
μ_0 = permeability of free space

Superscript

$( )^*$ = quantities evaluated at the sonic point

Received Aug. 9, 1985; presented as Paper 85-2039 at the AIAA/DGLR/JSASS 18th International Electric Propulsion Conference, Alexandria, VA, Sept. 30-Oct. 2, 1985; revision received Feb. 3, 1986.

*Assistant Professor, Mechanical Engineering; currently Senior Physicist, Space Power Inc., San Jose, CA. Member AIAA.
†Graduate Student, Mechanical Engineering Department.

I. Introduction

MAGNETOPLASMADYNAMIC (MPD) thrusters use electric and magnetic fields to accelerate a plasma to high speeds. Efficiencies of ~50% have been achieved but are limited by a destructive phenomenon known as "onset." This paper examines the plasma flow theoretically in a one-dimensional self-field thruster. The behavior of efficiency and its relationship to onset are considered. This theory predicts a new mechanism of onset related to the back-EMF. In this theory, onset appears as a conflict between the electric field required for magnetogasdynamic choking and the electric field necessary to draw all the applied current.

MPD thrusters, as distinguished from other electric propulsion devices, derive most of their thrust from $\boldsymbol{j}\times\boldsymbol{B}$ body forces in a steady flow.[1] The magnetic field may be externally applied as in some early work on the subject.[2-4] During the past ten years, work has concentrated on self-field thrusters. Operating at current levels of tens of kiloamps, self-field MPD thrusters have experimentally demonstrated exhaust speeds of 15,000 to 40,000 m/s and thrusts of the order of 100 N. This paper studies self-field thrusters.

For a given mass flow and geometry, it is experimentally known that efficiency increases rapidly as the current increases. This increase is limited by the rapid erosion that begins to occur at some current level. This limit, also typically associated with voltage oscillations, is known as "onset." For a given geometry and varying mass flow, this limit correlates with $J^2/\dot{m}$ where J is the total current and $\dot{m}$ the mass flow. This limit has been observed to vary with geometry[5,6] but this variation is not understood.

Equilibrium flow in an MPD thruster has been modeled by King et al.[7] They assume a one-dimensional, local equilibrium, continuum flow with a uniform and constant electric field. The fluid enters the thruster at a slow speed and low temperature, whereupon the speed increases to sonic primarily due to ohmic heating. The fluid is then accelerated to supersonic speeds primarily by the magnetic body force. The electric field is determined by the choking condition that permits a transition from subsonic to supersonic speeds. In this paper, the model of King et al.[7] will be considered for frozen and nonequilibrium flow. In a nonintuitive result, it will be found that the electric field required by the choking condition can be insufficient to draw all the applied current. This occurs at high values of $J^2/\dot{m}$ and is interpreted as onset.

Several previous explanations for onset have been advanced. In addition to the back-EMF theory presented here, there are two other approaches. The first deals with anode mass starvation and the second with current channel instability. Each will be reviewed.

The first approach, anode mass starvation, was first analyzed by Baksht et al.[8] Because of flow acceleration and the Hall effect, they predicted that the plasma density near the downstream portion of the anode would decline as total current increased. Consequently, as current increases, the anode sheath voltage will eventually shift signs, from electron-retaining to ion-retaining polarities. Bakst et al. took this sign change as their onset criterion.[8] This work has been refined by Heimerdinger.[9] Korsun considered a similar mass starvation effect in a two-dimensional model.[10] The anode mass starvation hypothesis has experimental support from Hugel.[11] The reason a change in sign of the anode sheath voltage should cause onset is not clear because many discharges operate in steady state with anode sheaths of both signs. Two hypotheses exist: 1) Kuriki and Onishi[12] suggest that when the anode fall is positive, ions accelerated in the sheath may produce sputtering, and 2) Shubin[13] found that anode mass starvation is associated not just with anode sheath reversal but also with plasma instabilities, and he suggested that these may cause onset.

The second approach to onset is being developed by Schrade et al.[14] They analyze the stability of current tubes to fluctuations in the magnetic field distribution. This is a volume rather than an electrode phenomenon.

The back-EMF theory differs fundamentally from the other two approaches. For one, the injection of a small amount of mass near the downstream end of the anode would have a major effect on the onset predictions of the anode mass starvation theories[8-10,13] but no effect on the back-EMF mechanism. Also, a fundamental difference between the back-EMF limit and the instability theories[13,14] is that the former appears in a steady-state model. Further, the magnetogasdynamic choking condition plays an essential role in the back-EMF mechanism but not in the other two theories. These differences indicate that the physical mechanisms for these approaches are different, but it is not yet known which mechanism occurs first and under which experimental conditions.

The most detailed experimental data on plasma flow conditions at onset come from the experiments of Barnett.[15] These experiments were conducted in what has become known as the "benchmark" thruster, which is characterized by a lip on the anode which protrudes into the flow channel. His experiments found instabilities associated with low density regions. Unlike Baksht et al.'s theory,[8] the low density region was not necessarily near the anode. These results have not yet been repeated in a thruster with a smoothy-shaped flow channel.

The complexity of this problem has prompted the use of some simplifying assumptions. Baksht et al.,[8] Shubin,[13] and Martinez-Sanchez and Heimerdinger[16] have used the isothermal assumption; Shubin[13] and Martinez-Sanchez and Heimerdinger[16] have used the infinite magnetic Reynolds number assumption. Neither approximation is used here; however, the Hall effect, which was partially included in the above models, will be neglected. This work, an extension of King et al.,[7] uses conservation of mass, momentum, and energy for a one-dimensional plasma flow. Unlike King et al.,[7] who assume equilibrium thermodynamics, this work also considers frozen-flow and nonequilibrium models. The choking condition is found to be strongly affected by these assumptions.

The governing equations of MPD channel flow is discussed in Sec. II. and magnetogasdynamic choking is presented in Sec. III. The solution for a constant composition, i.e. frozen, flow is derived in Sec. IV. Finally, Sec. V. uses the results of the frozen flow model to find a new mechanism for onset. The effect of ionization on this onset mechanism is discussed in Sec. VI., and a summary and conclusions are given in Sec. VII.

II. Governing Equations

A steady one-dimensional constant-area MPD channel flow is considered. The geometry is as shown in Fig. 1. Viscous effects are neglected. The governing equations can be written:

$$\text{mass: } \rho u = F = \text{const} \tag{1}$$

$$\text{momentum: } dP + F du = jB dx \tag{2}$$

$$\text{energy: } F dh + F u du = jE dx \tag{3}$$

$$\text{state: } h = h(P,\rho) \tag{4}$$

$$\text{Ohm's law: } j = \sigma(E - uB) \tag{5}$$

$$\text{Ampere's law: } \frac{dB}{dx} = -\mu_0 j \tag{6}$$

These can be understood as the equations of classical gasdynamics with the inclusion of ohmic heating in the energy Eq. (3) and a magnetic body force in the momentum Eq. (2).[17] The equation of state, Eq. (4), applies to nonideal as well as ideal gases. It will be generalized to nonequilibrium flow in Sec. VI.

First integrals can be found for both the momentum and energy equations. Using Ampere's law [Eq. (6)], momentum conservation [Eq. (2)] and energy conservation [Eq. (3)] become

$$\text{momentum: } P + Fu + (B^2/2\mu_0) = \text{const} \tag{7}$$

$$\text{energy: } Fh + (Fu^2/2) + (EB/\mu_0) = \text{const} \tag{8}$$

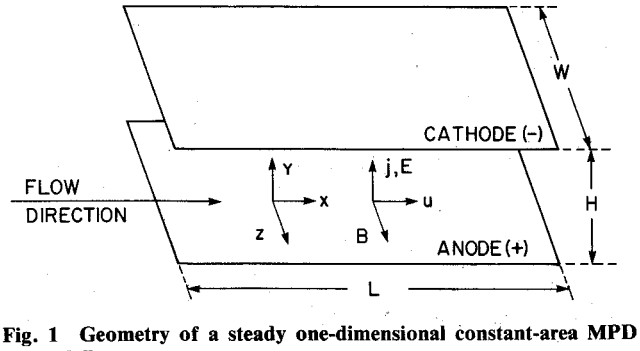

Fig. 1 Geometry of a steady one-dimensional constant-area MPD channel flow.

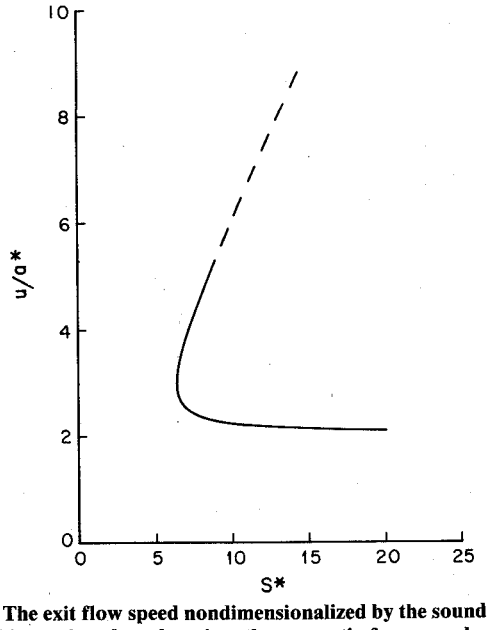

Fig. 2 The exit flow speed nondimensionalized by the sound speed at the choking point plotted against the magnetic force number S^*.

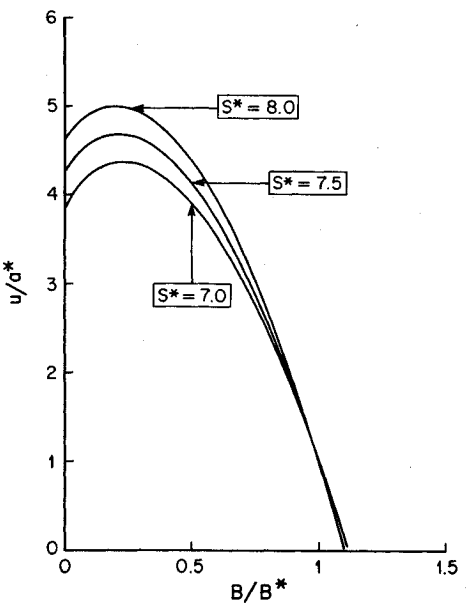

Fig. 2 The flow speed *un* plotted against the magnetic field *B* for three values of the magnetic force number *S.**

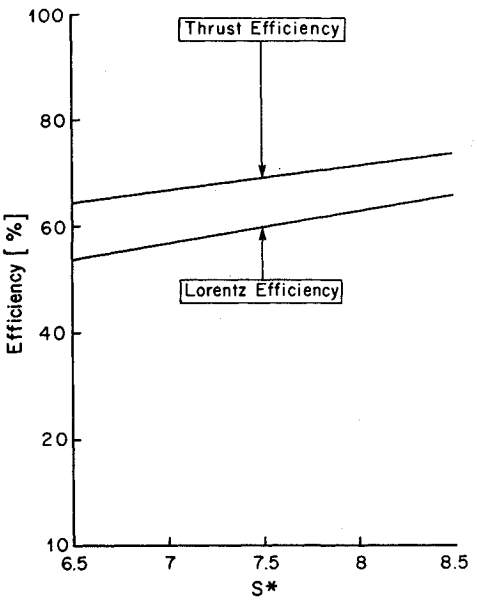

Fig. 4 The thrust efficiency η and Lorentz efficiency η_L plotted against the magnetic force number *S.**

To complete the problem description, boundary conditions are needed at the channel inlet, $x=0$, and exit, $x=L$. At $x=L$, we require $B=0$. At the inlet $x=0$, the flow speed is specified, $u=u_i$. The inlet flow speed, u_i is very small; and, for present purposes, it may be taken as approximately zero. The value of the magnetic field at the inlet $B=B_i$ is determined from the experimentally specified total current J by Ampere's law:

$$B_i=\mu_0 J/W \tag{9}$$

The mass flux F is related to the total mass flow $\dot{m}$ by:

$$F=\dot{m}/(HW) \tag{10}$$

The performance of the MPD thruster can be characterized by its efficiency. We will define two efficiencies. Although the definitions are different, they agree closely over the range of MPD operation. The first, inspired by thermodynamics, is the Lorentz efficiency, which is defined as the ratio of the work done by the electromagnetic force to the total electrical power in[7]

$$\eta_L=\int_0^L jBu\mathrm{d}x\Big/\int_0^L Ej\mathrm{d}x \tag{11}$$

When the integrand in Eq. (11) is rearranged, the Lorentz efficiency is seen to be the weighted average over the power of the ratio of the back-EMF to the electric field:

$$\eta_L=\int_0^L\left(\frac{uB}{E}\right)Ej\mathrm{d}x\Big/\int_0^L Ej\mathrm{d}x \tag{12}$$

$$=\left\langle\frac{uB}{E}\right\rangle \tag{13}$$

It is then evident from Eq. (13) that for efficient thruster operation it is necessary to operate in a regime where the back-EMF is comparable to the electric field. This means that the back-EMF onset mechanism, discussed in Sec. V., is expected to be important in efficient thrusters.

The second type of efficiency is conventionally used to define overall propulsion system performance:

$$\eta=(T_h^2/2\dot{m})/(JV) \tag{14}$$

where $T_h=(\dot{m}u+PHW)\,|_{x=L}$ is the total thrust. For a planar channel, $V=EH+V_s$ where V_s is the sum of the sheath voltage drops. By including the thrust due to pressure, η differs from η_L. For the normal operating regime of MPD thrusters, as opposed to electrothermal thrusters, the pressure component of thrust is small and the two efficiencies agree closely, as will be shown in Sec. IV.

The governing equations described in this section can be solved to determine the electrical characteristics and efficiency of the thruster. This will be done in the following sections.

III. Magnetogasdynamic Choking

The combined action of ohmic heating and Lorentz body force can cause a flow in a constant-area channel to accelerate from subsonic to supersonic. Since both of these effects are large in the MPD thruster, variation in the channel cross-sectional area may be unimportant even if it is present. This section will develop the condition for this choking to occur in the self-field flow of a nonideal gas obeying equation of state Eq. (4).

Rewriting Eqs. (1) and (4) in differential form, combining them with Eqs. (2) and (3) to eliminate $\mathrm{d}p$ and $\mathrm{d}\rho$, using Eq. (5) to eliminate j, and solving for the velocity gradient yields

$$\frac{1}{u}\frac{\mathrm{d}u}{\mathrm{d}x}=\frac{1}{M^2-1}\frac{1}{\rho\partial h/\partial\rho\,|_P}\left(\frac{B}{\mu_0}\frac{\partial h}{\partial P}\bigg|_\rho-\frac{E}{\mu_0\rho u}\right)\frac{\mathrm{d}B}{\mathrm{d}x} \tag{15}$$

where $M=u/a$ is the Mach number and a is given by[18]

$$a^2=(\rho\partial h/\partial\rho\,|_P)/(1-\rho\partial h/\partial P\,|_\rho) \tag{16}$$

a is the acoustic speed of sound in a gas obeying equation of state Eq. (4).[18] For the special case of an ideal gas, Eq. (16) reduces to the conventional expression.

It is seen that Eq. (15) is singular at $M=1$. For continuous acceleration through $M=1$, it is required that

$$E=\rho^*a^*B^*\frac{\partial h}{\partial P}\bigg|_{\rho^*} \tag{17}$$

where * represents quantities evaluated at the sonic point, $M=1$. Equation (17) is the choking condition. It relates the

electric field E to the back-EMF at the choking point, a^*B^*. This will play a central role in the prediction of back-EMF induced onset discussed in Sec. V.

Equation (17) can be interpreted in terms of classical gasdynamics. Ohmic heating tends to drive a gas toward $M=1$ and the magnetic body force tends to drive the flow away from $M=1$.[17] Equation (17) determines the electric field necessary to provide the right amount of ohmic heating to drive the flow just to $M=1$ where the body force can accelerate it to supersonic speeds.

This choking condition has been previously studied for the special case of an ideal gas. Resler and Sears[19,20] considered such choking for an applied-field calorically-perfect flow. King et al.[7] studied choking in self-field flow for the special case of a gas obeying the equation of state $h=h(P/\rho)$. The case of a self-field calorically-perfect flow will be considered in the next section, and the more general case of self-field choking in a nonideal gas will be addressed in Sec. VI.

IV. Frozen Flow Model

The concept of back-EMF onset is most easily understood in the special case of a constant-composition (frozen) calorically perfect plasma. In this section, the solution for the flow profiles for frozen flow is presented. The flow in this case is found to be characterized by a single nondimensional parameter. This parameter, the magnetic force number, is closely related to the experimental onset parameter $J^2/\dot{m}$.

The flow of a fully-ionized one-temperature plasma is modeled. Because ionization and recombination reaction rates are not considered in this section, this is called the frozen flow model. With electronic excitation neglected, this assumption of a fully ionized flow permits a simple expression for enthalpy:

$$h=\frac{5kT}{m_A}+\frac{\epsilon_i}{m_A}=\frac{5P}{2\rho}+\frac{\epsilon_i}{m_A} \tag{18}$$

Substituting this frozen flow enthalpy into the choking condition, Eq. (17), gives

$$E=\frac{5}{2}a^*B^* \tag{19}$$

This choking condition determines the electric field and defines the operating region.

To obtain an analytic solution, the conservation equations for mass [Eq. (1)], momentum [Eq. (7)], and energy [Eq. (8)] may be rewritten for frozen flow in terms of the sonic quantities:

$$\rho u=F=\rho^*a^* \tag{20}$$

$$P+Fu+\frac{B^2}{2\mu_0}=P^*+Fa^*+\frac{B^{*2}}{2\mu_0} \tag{21}$$

$$Fh+F\frac{u^2}{2}+\frac{EB}{\mu_0}=Fh^*+F\frac{a^{*2}}{2}+\frac{EB^*}{\mu_0} \tag{22}$$

Combining Eqs. (18–22), the following quadratic equation for u is obtained:

$$u^2+\left(\frac{5}{8}S^*\left(\frac{B^2}{B^{*2}}-2\right)-2\right)a^*u + \left(\frac{5}{4}S^*\left(1-\frac{B}{B^*}\right)+1\right)a^{*2}=0 \tag{23}$$

where

$$S^*=B^{*2}/(\mu_0\rho^*a^{*2}) \tag{24}$$

The two solutions to quadratic Eq. (23) may be readily written in terms of B and the sonic quantities

$$u=a^*\left[-\frac{\zeta}{2}\pm\frac{(\zeta^2-4\xi)^{1/2}}{2}\right] \tag{25}$$

where

$$\zeta=\frac{5}{8}S^*\left(\frac{B^2}{B^{*2}}-1\right)-2, \qquad \xi=\frac{5}{4}S^*\left(1-\frac{B}{B^*}\right)+1$$

The upper sign in Eq. (25) represents the solution for supersonic flow and the lower sign is for subsonic flow. Eq. (25) shows that u/a^* is a function of B/B^* with S^* as a parameter. Combining Eq. (25) with conservation of mass Eq. (20), ρ can be found:

$$\rho=\rho^*\left[-\frac{\zeta}{2}\pm\frac{(\zeta^2-4\xi)^{1/2}}{2}\right]^{-1} \tag{26}$$

Eq. (26) determines ρ/ρ^* as a function of B/B^* with S^* as a parameter. Combining Eq. (25) with momentum conservation Eq. (21), the pressure P can be found:

$$P=Fa^*\left[\frac{8}{5}+\frac{\zeta}{2}\mp\frac{(\zeta^2-4\xi)^{1/2}}{2}+\frac{S^*}{2}\left(1-\frac{B^2}{B^{*2}}\right)\right] \tag{27}$$

Eq. (27) determines P/Fa^* as a function of B/B^* with S^* as a parameter. The relationship between B and position x can be found by combining Ohm's law [Eq. (5)], Ampere's law [Eq. (6)], and choking condition [Eq. (19)]:

$$\frac{dB}{dx}=-\mu_0\sigma\left(\frac{5}{2}a^*B^*-uB\right) \tag{28}$$

From Eqs. (25–27), it is seen that S^*, defined by Eq. (24), is a very important parameter. S^* is the magnetic force number[21] evaluated at the choking point, and displays the relative importance of magnetic pressure and gas dynamic kinetic energy density:

$$S^*=\frac{B^{*2}/2\mu_0}{1/2\rho^*a^{*2}}=\frac{\text{magnetic pressure}}{\text{kinetic energy density}} \tag{29}$$

This magnetic force number S^* is very closely related to the onset parameter $J^2/\dot{m}$, which is used by experimentalists to correlate data. Using Ampere's law [Eq. (9)], mass flux definition [Eq. (10)], and the definition of S^*, [Eq. (24)] yields

$$\frac{J^2}{\dot{m}}=\left(\frac{\mathcal{R}a^*}{\mu_0\kappa^2}\right)S^* \tag{30}$$

where $\kappa=B_i/B^*$ is typically about 1.1.[7]

Limits on operating values of S^* can quickly be established. First, for Eq. (25) to have a real solution, it is necessary that $\zeta^2>4\xi$. This occurs for the trivial case of $S^*=0$ or $S^*>6.4$. For a physical solution, it is also necessary that $P>0$. Examination of Eq. (27) shows that this limits S^* to values less than 14.0. In light of Eq. (30), this upper limit on S^* could signify onset. In the next section, however, a more severe limit than $S^*<14.0$ will be found.

The behavior of these solutions is illustrated in several figures. Figure 2 shows the variation of the nondimensional exit speed (u_e/a^*) vs the parameter S^*. The top portion of the curve represents the supersonic branch of the solution, whereas the bottom portion gives the subsonic branch. The supersonic flow profiles for three values of S^* are shown in Fig. 3. The thruster efficiency for the supersonic flow branch

is shown in Fig. 4. This figure shows that the two definitions for efficiency presented in Sec. II are in close agreement.

In summary, analytical relations between u, ρ, P and B have been found. The solutions contained S^*, the magnetic force number evaluated at the choking point, as a parameter. The solution was found assuming a fully-ionized compositionally-frozen flow. Approximations such as isothermal flow or infinite magnetic Reynolds number have *not* been made. The next section reveals how this solution predicts a new mechanism of onset. In Sec. VI, how the solution is affected by ionization rates is discussed.

V. Onset

This section explains how the simple model of the previous section predicts onset. Onset appears as a limitation on the values S^*, as defined in Eq. (24) or Eq. (29), may assume in the supersonic mode. This limit is a consequence of combining Ohm's law with the flow solutions. The behavior of the back-EMF will be considered first. The effect of back-EMF on Ohm's law is then considered from mathematical and physical viewpoints.

The behavior of the back-EMF, uB, is considered first. Near the inlet, the flow speed u is very small, so uB is small. Near the exit, uB is again small because $B \to 0$. Somewhere near the middle of the thruster, the back-EMF, uB, peaks. This is shown in Fig. 5 for various values of S^*.

An important relationship between the electric field E and the back-EMF uB can be found if Ohm's law is considered. Combining Ohm's law [Eq. (5)] with Ampere's law [Eq. (6)] and integrating yields

$$L = \int_0^{B_i} \frac{dB}{\mu_0 \sigma (E - uB)} \tag{31}$$

where L is the thruster length, B_i the magnetic field at $x=0$, and σ the plasma electrical conductivity. The relationship between u and B is given by Eq. (25). For frozen flow, the electric field E is given by the choking condition [Eq. (19)]. This is also plotted in Fig. 5. From Fig. 5, it is seen that as S^* increases from 7.0 to 8.5, the peak back-EMF approaches the electric field. This tends to make the denominator in Eq. (31) small. As the peak back-EMF reaches the electric field, the integral indicates that an infinite length thruster is necessary. This occurs at $S^* = 8.52$. For higher S^*, $E - uB$ changes sign twice during the integral, which is hence singular and meaningless.

The physical significance of this limit can be found by returning to the governing equations, Eqs. (1-6). If at some location in the thruster $E = uB$, then from Ohm's law, [Eq. (5)] no current flows. If no current flows, no magnetic force acts on the plasma [see Eq. (7)] and no ohmic heating occurs [see Eq. (8)]. Consequently, the plasma flows at constant speed and temperature. Further, if no current flows, the magnetic field is constant [see Eq. (6)]. All this implies that if $E = uB$ somewhat in the channel, then it will be true that $E = uB$ at all points downstream. If this is so, the boundary condition of $B = 0$ at $x = L$ cannot be met no matter how long the thruster. Thus, it is necessary that $uB < E$ for all locations within the channel.

The limit of $uB < E$ for the analogous case of plasma accelerators with *applied* magnetic fields is well-known. It was first studied by Resler and Sears[19,20] and has since appeared in textbooks.[21,22]

This value of $S^* = 8.52$ at which $E = uB$ can therefore be considered as the onset limit, indicating a regime of operation beyond which the flow can no longer be supersonic. Using Eq. (30), this limit can be restated dimensionally:

$$\frac{J^2}{\dot{m}} \leq 8.52 \frac{\mathcal{R} a^*}{\mu_0 \kappa^2} \tag{32}$$

Eq. (32) correlates the experimental data of Malliaris et al.[5] very well. This is shown in Fig. 6. This success does not prove the existence of back-EMF onset, however, because the scaling laws for anode mass starvation onset[8,9] are similar.

The reason back-EMF should rise faster than the electric field can be explained with some scaling behavior. From Ampere's law [Eq. (6)] B scales directly with J. From the choking condition [Eq. (17)] E scales roughly with J, and from conservation of momentum [Eq. (2)], u scales roughly with $J^2/\dot{m}$. Thus, as one increases the current, the back-EMF, which scales as $J^3/\dot{m}$, increases faster than E, which scales as J. This leads ultimately to current blocking.

This paper does not attempt to establish the flow conditions after onset has occurred. For $S^* > 8.52$, the smoothly accelerating supersonic solution discussed in Sec. IV is not possible. Thus, some largely subsonic flow is expected. By energy conservation [Eq. (8)], a subsonic flow would likely

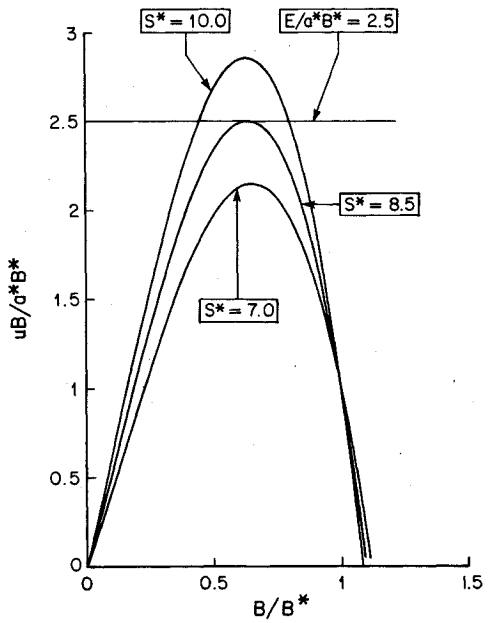

Fig. 5 The back-EMF uB plotted against the magnetic field B for three values of the magnetic force number S^* for supersonic flow.

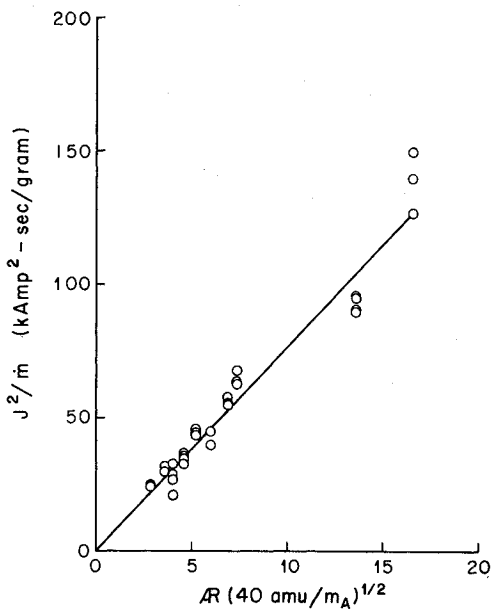

Fig. 6 The experimental data of Malliaris et al.[5] for onset conditions correlate as predicted by back-EMF onset theory.

have a higher temperature. Thus higher erosion rates, by evaporation as well as by sputtering, are expected.

Back-EMF onset also affects the efficiency. It was shown earlier in Eqs. (12) and (13) that for thruster operation with a high Lorentz efficiency, it is necessary to operate in a regime with a high average value of uB/E. Since back-EMF onset restricts the peak value of uB/E to one, its average must be much less (see Fig. 5). Thus, back-EMF onset restricts the efficiency as well as S^*.

VI. Effect of Ionization

The previous section considered back-EMF onset quantitatively in the frozen flow model. In this section, the effect of non-zero ionization rates is included. This is done first under the equilibrium and secondly under the nonequilibrium assumptions. It is found that ionization rates have a strong effect on the choking condition and thus on the appearance of back-EMF onset.

For both the frozen flow and equilibrium flow limits, the magnetogasdynamic choking condition can be written as

$$\frac{E}{a^*B^*}=\rho^*\frac{\partial h}{\partial P}\bigg|_{\rho^*} \tag{33}$$

For frozen flow of a monatomic gas, the right-hand side of Eq. (33) has the value of 5/2. The equilibrium calculation causes the right-hand side of Eq. (33) to be up to an order of magnitude larger. This is shown in Fig. 7. The major difference between the two limits is that an important part of the change in enthalpy in equilibrium is due to the change in the ionization fraction. The right-hand side of Eq. (33) oscillates in the equilibrium model as the plasma progresses through successive ionization stages.

The difference in thermodynamics has an important effect on back-EMF onset. Since the equilibrium model can predict large electric fields, the occurrence of back-EMF blocking is delayed. This is why King et al.[7] did not find evidence of onset over the range of parameters used in their numerical calculation.

The nature of the choking condition with nonequilibrium ionization can be analyzed as follows. A plasma composed of electrons, neutrals, and once-ionized ions is considered. In nonequilibrium, the equation of state [Eq. (4)] must be replaced by

$$h=h(P,\rho,\alpha) \tag{34}$$

where α is the ionization fraction. Proceeding exactly as before, we can combine the governing equations in differential form with the new equation of state Eq. (34), solve for the velocity gradient, and obtain the following nonequilibrium choking condition:

$$E=\rho^*a^*B^*\frac{\partial h}{\partial P}\bigg|_{(\rho^*,\alpha^*)}+\frac{\rho^*a^*}{j^*}\frac{\partial h}{\partial \alpha}\bigg|_{(P^*,\rho^*)}\frac{\mathrm{d}\alpha}{\mathrm{d}x}\bigg|_{x=x^*} \tag{35}$$

where $(\,)^*$ refers to quantities evaluated at the sonic point. The above shows the effect of ionization rates on the electric field explicitly.

Neglecting again electronic excitation, an analytic form for the equation of state can be found:

$$h=h(P,\rho,\alpha)=(5P/2\rho)+(\alpha\epsilon_i/m_A) \tag{36}$$

Using Eq. (36), the choking condition Eq. (35) may be simplified to

$$E=\frac{5}{2}a^*B^*+\frac{\rho^*a^*\epsilon_i}{j^*m_A}\frac{\mathrm{d}\alpha}{\mathrm{d}x}\bigg|_{x=x^*}$$

Observe that the first term on the right-hand side is the electric field from the frozen flow theory and the second term represents the dependence of the electric field on the ionization rate at the sonic point. The physical significance of the relative magnitude of these two terms can be found by rewriting the above equation in the following nondimensional form:

$$\frac{E}{a^*B^*}=\frac{5}{2}+\frac{\rho^*\epsilon_i}{j^*B^*m_A}\frac{\mathrm{d}\alpha}{\mathrm{d}x}\bigg|_{x=x^*} \tag{37}$$

Consider a unit volume of the plasma as it travels a distance $\mathrm{d}x$. $(\rho^*\epsilon_i/m_A)\mathrm{d}\alpha$ is the energy added to ionization. $jB\mathrm{d}x$ is the work done by the magnetic field to accelerate the plasma. Thus, the second term on the right of Eq. (37) measures the ratio of energy going into ionization to the work done in accelerating the plasma.

The ionization rate $\mathrm{d}\alpha/\mathrm{d}x$ is found in a nonequilibrium model from a rate equation:

$$\frac{\mathrm{d}\alpha}{\mathrm{d}x}=\frac{k_f\rho\alpha(1-\alpha)}{m_Au}-\frac{k_b\rho^2\alpha^3}{m_A{}^2u}$$

The frozen flow model is found as the limit in which k_f and k_b approach zero. If k_f and k_b approach infinity, the equilibrium model is recovered.

In this section, the choking condition for frozen and equilibrium flow have been compared. Fig. 7 showed a large quantitative difference between these two limits. Using a generalized equation of state [Eq. (34)], the magnetogasdynamics choking condition was extended to non-equilibrium flow in Eq. (35). It was shown that the importance of the ionization term in the choking condition was determined by the relative rate at which energy enters ionization to the rate at which work is done on the flow at the choking point.

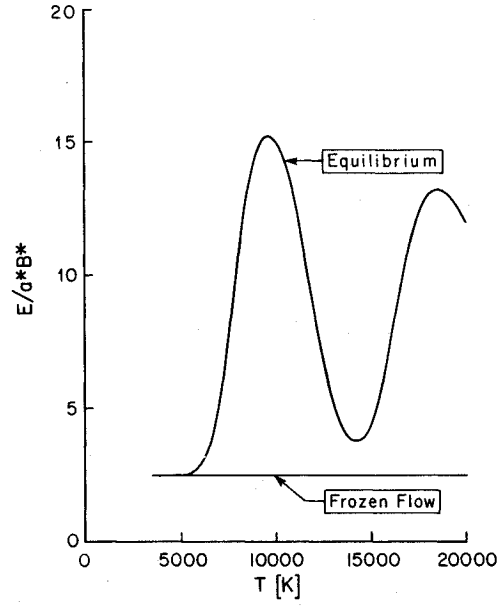

Fig. 7 The electric field determined by the choking condition, Eq. (17), plotted against temperature at the choking point for the two cases of equilibrium and frozen flow.

VII. Summary and Conclusions

A model of one-dimensional plasma flow in the MPD thruster has been presented. Three different thermodynamic models have been used: frozen flow, equilibrium flow, and nonequilibrium flow. Because of its simplicity, an analytical solution was found for the frozen flow case. A single parameter, S^*, governed the solution. S^* was shown to be proportional to the well-known experimental parameter $J^2/\dot{m}$. Onset appeared in this model through the nonintuitive result that, for a sufficiently large S^*, the electric field is insufficient

to draw the applied current in the supersonic mode. For frozen flow, the onset criterion was given by Eq. (32). When ionization occurs, such as in an equilibrium or nonequilibrium flow, onset is delayed because the choking condition predicts a larger electric field. This explains why, over the parameter range they studied, King et al.[7] did not observe back-EMF onset in their numerical results for equilibrium flow. No simple analytic solution was found when ionization occurs.

The cause of back-EMF onset can be traced to two physical phenomena. The first is magnetogasdynamic choking which relates the electric field to the back-EMF at the choking point. The second is the requirement that $E-uB$ not change sign in the thruster. If the latter is violated, it is not possible to draw all the current in a finite length thruster. Both these requirements are well-known for the case of applied-field accelerators.[19-22] This paper has shown that the combination of these two in a self-field flow limits the current that may be applied in one-dimensional supersonic flow.

The back-EMF mechanism of onset is distinctly different from the anode mass starvation hypothesis.[8-11,13] This is physically clear when considering injection of a small amount of mass through the downstream portion of the anode. Such mass injection could have a major effect on the possibility of anode mass starvation but no effect on the back-EMF onset mechanism.

This work, like that of King et al.,[7] shows the significance of considering conservation of energy, [Eq. (3)]. Without differential conservation of energy, as in the isothermal models, choking conditions such as Eq. (17) or Eq. (35) are not found. This changes the electrical characteristics of MPD thrusters. Further experimental information on the choking region would be valuable.

Acknowledgments

The authors acknowledge helpful discussions with D. Q. King. This work was supported by AFOSR-83-0033.

References

[1]Jahn, R.G., *Physics of Electric Propulsion*, McGraw-Hill Book Company, New York, 1968.

[2]Sherman, A., "Theoretical Performance of a Crossed Field MHD Accelerator," *ARS Journal*, Vol. 32, March 1962, pp. 414-420.

[3]Workman, J.B., "Arc Structure in a Magnetic Annular Discharge," *AIAA Journal*, Vol. 7, March 1969, pp. 512-519.

[4]Chubb, D.L., "Fully Ionized Quasi-One-Dimensional Magnetic Nozzle Flow," *AIAA Journal*, Vol. 10, Feb. 1972, pp. 113-114.

[5]Malliaris, A.C., John, R.R., Garrison, R.L., and Libby, D.R., "Performance of Quasi-Steady MPD Thrusters at High Powers," *AIAA Journal*, Vol. 10, Feb. 1972.

[6]King, D.Q., Smith, W.W., Jahn, R.G., and Clark, K.E., "Effect of Thrust Chamber Configuration on MPD Arcjet Performance," *Proceedings of the Princeton/AIAA/DGLR 14th International Electric Propulsion Conference.*

[7]King, D.Q., Clark, K.E., and Jahn, R.G., "Effect of Choked Flow on Terminal Characteristics of MPD Thrusters," AIAA Paper 81-0686, April 1981.

[8]Baksht, F.G., Moizhes, B. Ya., and Rybakov, A.B., "Critical Regime of a Plasma Accelerator," *Soviet Physics Technical Physics*, Vol. 18, No. 12, 1974, pp. 1613-1616.

[9]Heimerdinger, D.J., "An Approximate Two-Dimensional Analysis of an MPD Thruster," Master's Thesis, Massachusetts Institute of Technology, June 1984.

[10]Korsun, A.G., "Current Limiting by Self Magnetic Field in a Plasma Accelerator," *Soviet Physics Technical Physics*, Vol. 19, No. 1, 1974, pp. 124-126.

[11]Hugel, H. "Effect of Self-Magnetic Forces on the Anode Mechanism of a High Current Discharge," *IEEE Transactions on Plasma Science*, Vol. PS-8, No. 4, 1980, pp. 437-442.

[12]Kuriki K., Onishi, M., and Mormato, S., "Thrust Measurement of KIII MPD Arcjet," *AIAA Journal*, Vol. 20, 1982, pp. 1414-1419.

[13]Shubin, A.P., "Dynamic Nature of Critical Regimes in Steady-State High-Current Plasma Accelerators," *Soviet Journal of Plasma Physics*, Vol. 2, 1976, pp. 18-21.

[14]Schrade, H.O., Auweter-Kurtz, M., and Kurtz, H.L., "Stability Problems in Magnetoplasmadynamic Arc Thrusters," *18th Fluid Dynamics and Plasmadynamics and Laser Conference*, Cincinnati, OH, 1985.

[15]Barnett, J., *Operation of the MPD Thruster with Stepped Current Input*, Ph.D. Dissertation, Princeton University, Princeton, NJ, 1985.

[16]Martinez-Sanchez, M., Heimerdinger, D.J., "Analysis of Performance Limiting Factors in MPD Thrusters," *IEEE International Conference on Plasma Science*, Pittsburgh, PA, 1985.

[17]Shapiro, A.H., *The Dynamics and Thermodynamics of Compressible Fluid Flow*, Ronald Press, New York, 1953.

[18]Vincenti, W.G., and Kruger, C.H., *Introduction to Physical Gas Dynamics*, John Wiley and Sons, New York, 1967.

[19]Resler, E.L. Jr., and Sears, W.R., "The Prospects for Magneto-Aerodynamics," *Journal of the Aeronautical Sciences*, Vol. 25 April 1958, pp. 235-245.

[20]Resler, E.L. Jr., and Sears, W.R., "Magneto-Gasdynamic Channel Flow," ZAMP, Vol. IXb, 1958, pp. 509-519.

[21]Sutton, G.W., and Sherman, A. *Engineering Magnetohydrodynamics*, McGraw-Hill Book Co., New York, 1965.

[22]Hughes, W.F., and Young, F.J., *The Electromagnetodynamics of Fluids*, John Wiley & Sons, Inc., New York, 1966.